BIOLOGY OF REPRODUCTION **70,** 925–935 (2004)
Published online before print 19 November 2003.
DOI 10.1095/biolreprod.103.020941

Regulation of Ribosomal RNA Synthesis During the Final Phases of Porcine Oocyte Growth[1]

Bolette Bjerregaard,[3] Christine Wrenzycki,[4] Vlada V. Philimonenko,[5] Pavel Hozak,[5] Jozef Laurincik,[7,8] Heiner Niemann,[4] Jan Motlik,[6] and Poul Maddox-Hyttel[2,3]

Department of Anatomy and Physiology,[3] Royal Veterinary and Agricultural University, 1870 Frederiksberg, Denmark
Department of Biotechnology,[4] Institute for Animal Science (FAL), Mariensee, 31535 Neustadt, Germany
Institute of Experimental Medicine[5] and Institute of Animal Physiology and Genetics,[6] Academy of Sciences of Czech Republic, Prague, Czech Republic
Constantin the Philosopher University,[7] Nitra, Slovak Republic
Research Institute of Animal Production,[8] Nitra, Slovak Republic

ABSTRACT

In porcine oocytes, acquisition of meiotic competence coincides with a decrease of general transcriptional activity at the end of the oocyte growth phase and, specifically, of ribosomal RNA (rRNA) synthesis in the nucleolus. The present study investigated the regulation of rRNA synthesis during porcine oocyte growth. Localization and expression of components involved in regulation of the rRNA synthesis (the RNA polymerase I-associated factor PAF53, upstream binding factor [UBF], and the pocket proteins p130 and pRb) were assessed by immunocytochemistry and semiquantitative reverse transcription-polymerase chain reaction and correlated with ultrastructural analysis and autoradiography following [^{3}H]uridine incubation in growing and fully grown porcine oocytes. In addition, meiotic resumption, ultrastructure, and expression of p130, UBF, and PAF53 were analyzed in growing and fully grown porcine oocytes cultured with 100 μM butyrolactone I (BL-I), a potent inhibitor of cyclin-dependent kinases, to gain insight concerning the regulation of rRNA transcription during meiotic arrest. Immunocytochemical analysis demonstrated that p130 became colocalized with UBF and PAF53 and that the intensity of the PAF53 labeling decreased toward the end of the oocyte growth phase. These data suggest that the decrease in rRNA synthesis is regulated through inhibition of UBF by p130 as well as by decreased availability of PAF53. Moreover, expression of mRNA encoding PAF53 was decreased at the end of the oocyte growth phase. At the morphological level, these events coincided with inactivation of the nucleolus, as visualized by the transformation of the fibrillogranular nucleolus to an electron-dense fibrillar sphere with remnants of the fibrillar centers at the surface. Meiotic inhibition with 100 μM BL-I had a detrimental effect on the ability of porcine oocytes to resume meiosis and on nucleolus morphology, resulting in a lack of RNA synthetic capability as the fibrillar components, where rRNA transcription and initial processing occur, condensed or even disintegrated.

follicular development, gamete biology, oocyte development

INTRODUCTION

In vitro production of porcine embryos, including in vitro maturation (IVM) of oocytes followed by in vitro fertilization and in vitro culture, may result in live offspring, but it is still associated with great inefficiencies [1]. Prevalent problems are a high proportion of polyspermic fertilization and low numbers of developmentally competent blastocysts [2]. These problems are thought to result mainly from insufficient cytoplasmic maturation of the oocyte in vitro [3]. It has been demonstrated in mice [4], goats [5], sheep [6], and cattle [7] that the oocyte, during folliculogenesis, progressively acquires the ability to resume and progress through meiosis and to sustain embryonic development. The ability to resume meiosis (i.e., to undergo germinal vesicle breakdown [GVBD]) is acquired by porcine oocytes when they approach the end of the growth phase in antral follicles greater than 0.8 mm in diameter, which is well before they acquire the capacity for completing meiotic maturation to metaphase II at a follicular diameter of greater than 2 mm [8, 9]. Acquisition of full meiotic competence coincides with a markedly decreased rate of transcription in the oocyte and a complete inactivation of the ribosomal RNA (rRNA) synthesis in the nucleolus of the gamete [10, 11].

Transcription of the rRNA genes and the subsequent processing of rRNA to the formation of preribosomal particles are spatially organized within the nucleolus [12]. The three major nucleolar compartments are the fibrillar centers (FCs), the surrounding dense fibrillar component (DFC), and the granular component (GC; for review, see [13]). The FCs harbor the enzymatic machinery for the transcriptional process, the DFC carries the primary nascent transcript, and the GC represents processed transcripts associated with proteins in the form of preribosomal particles. Initiation of transcription of the rRNA genes requires the formation of the transcription initiation complex, consisting of RNA polymerase I (RNA Pol I), RNA Pol I-associated factors, and at least two specific transcription initiation factors, the species-specific selectivity factor 1 (SL-1) and the upstream binding factor (UBF) (Fig. 1) [14, 15].

Formation of the transcription initiation complex requires interaction between RNA Pol I and an RNA Pol I-associated factor, PAF53, which promotes the interaction between RNA Pol I and UBF (Fig. 1) [16]. The mechanism by which UBF activates rRNA gene transcription involves formation of dimers [17], binding of UBF to the upstream promoter element of the rRNA genes [18], and interaction between UBF and the rRNA gene transcription initiation

[1]Supported by grants from the Danish Research Agency (9901178), NATO (978658), the Deutsche Forschungsgemeinschaft (DFG), the Grant Agency of the Academy of Sciences of the Czech Republic (IAA5039202) to P.H., and an institutional grant (AV0Z5039906) to P.H.
[2]Correspondence: Poul Maddox-Hyttel, Department of Anatomy and Physiology, Royal Veterinary and Agricultural University, Groennegaardsvej 7, DK-1870 Frederiksberg C, Denmark. FAX: 45 3528 2547; e-mail: poh@kvl.dk

Received: 7 July 2003.
First decision: 28 July 2003.
Accepted: 21 October 2003.

ISSN: 0006-3363. http://www.biolreprod.org

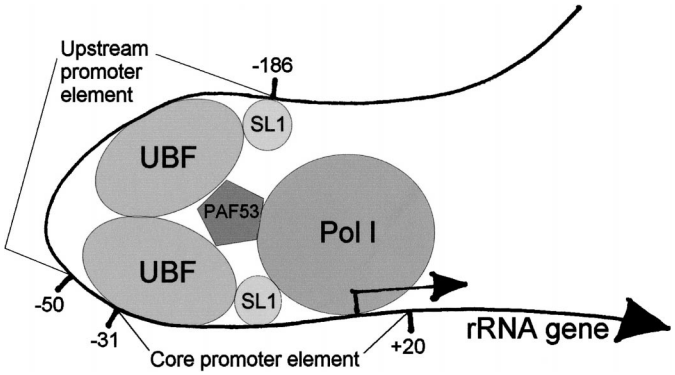

FIG. 1. Schematic depiction of the transcription initiation complex on the rRNA gene promoter. The factors include UBF, SL-1, PAF53, and RNA Pol I. The UBF binds to the promoter as a dimer and bends the rRNA gene promoter. Additionally, UBF binds SL-1 and brings it to the core element, leading to transcriptional activation. The PAF53 is associated with RNA Pol I and UBF.

factor SL-1 [19]. SL-1 is a multimeric protein containing the TATA-binding protein (TPB) and at least three TPB-associated factors that are specific for transcription by RNA Pol I [20]. The rRNA gene promoters lack a TATA-box, and SL-1, by itself, does not bind to the rRNA gene core promoter element [21]. Therefore, binding of SL-1 is mediated through interaction with UBF [22]. Once bound to UBF, SL-1 is in direct contact with the rRNA gene promoter and directs promoter-specific initiation of transcription and, thereby, rRNA synthesis.

Synthesis of rRNA plays a key role in the maintenance of cell function and is closely correlated with the growth and cell-cycle state [23]. In somatic cells, the growth-dependent control of rRNA synthesis is primarily mediated by posttranslational modifications, such as phosphorylation, of basal transcription factors, such as UBF. The activity of UBF and, thus, rRNA synthesis can also be altered by the so-called pocket proteins. The retinoblastoma family of pocket proteins includes the tumor-suppressor pRb and the related p130 and p107 multifunctional proteins, which are involved in cell-cycle regulation, cell growth, cell differentiation, and cell death [24, 25]. Recently, both p130 and pRb were found to inhibit rRNA synthesis through direct binding of UBF [26–29].

The molecular mechanism by which rRNA gene transcription is downregulated toward the end of the oocyte growth phase is, to a large extent, unknown. Therefore, the goal of the present study was to examine the nucleolar ultrastructure and RNA synthetic capacity in growing and fully grown porcine oocytes and, in parallel, to analyze the mRNA expression and location of UBF and PAF53 as well as the pocket proteins pRb and p130.

To gain insight concerning the relationship between the regulation of rRNA transcription and the mechanisms controlling the meiotic cell cycle, we employed the cell cycle-inhibitor butyrolactone I (BL-I), which inhibits cyclin-dependent kinases (cdks) in bovine and porcine oocytes, resulting in arrest at the germinal vesicle (GV) stage [30–33]. In growing bovine oocytes, the meiotic arrest induced by BL-I correlated with a decrease in RNA synthesis and changes of the nucleolus morphology. To our knowledge, the effect of BL-I on RNA synthesis and nucleolus ultrastructure in porcine oocytes has not been examined and, therefore, was included in the present investigation.

MATERIALS AND METHODS

The chemicals were purchased from Sigma Chemical Co. (St Louis, MO) unless otherwise indicated.

Oocyte Collection

Follicles were dissected from porcine ovaries obtained from a slaughterhouse and divided into the following four categories according to their diameter: small (0.3–0.7 mm), medium-small (0.8–1.2 mm), medium-large (1.8–2.2 mm), and large (3–5 mm). Follicles were then placed into Petri dishes with basic culture medium (BM) of the following composition: TCM 199, 0.75% $NaHCO_3$, 9.5 mM Hepes, 1.82 mM sodium pyruvate, 50 IU/ml of penicillin K salt, 50 IU/ml of streptomycin sulfate, and 125 ng/ml of amphotericin B. Oocytes were isolated from follicles with fine forceps and preparation needles, then picked up and transferred to different culture media. For general culture of oocytes, BM was supplemented with 3 mg/ml of polyvinyl alcohol (BM-PVA). The oocytes incubated with or without BL-I were distributed for 1) [^{3}H]uridine incubation, autoradiography, and transmission electron microscopy (TEM); 2) whole-mount immunolabeling; or 3) reverse transcription-polymerase chain reaction (RT-PCR).

Incubation with BL-I

In the experiment specifically examining the cell-cycle arrest on the RNA activity, cumulus-oocytes complexes (COCs) from small, medium-small, and large follicles were allocated to 500 μl of BM-PVA supplemented with 100 μM BL-I (Funakoshi, Tokyo, Japan), referred to hereafter as meiosis-inhibiting medium (MIM), and cultured in four-well Nunclon dishes (Roskilde, Denmark) under mineral oil for 24 h. Subsequently, COCs were washed four times in BL-I-free BM and submitted to IVM in TCM 199 maturation medium (MM; TCM 199, 10% fetal calf serum, 0.75% $NaHCO_3$, 9.5 mM Hepes, 200 mM L-glutamine, 50 IU/ml of penicillin K salt, 50 IU/ml of streptomycin sulfate, and 1 IU/ml of FSH) for 44 h. A control group of COCs from large follicles was submitted to IVM in MM for 44 h directly after isolation. At the end of the 44-h maturation culture, COCs were harvested for analysis of nuclear maturation by acetoorcein staining. For study of nucleolus morphology and RNA synthetic capacity, COCs from small, medium-small, and large follicles were harvested from the MIM culture at 4 and 24 h and processed for [^{3}H]uridine incubation, autoradiography, and TEM. Furthermore, COCs harvested at 24 h were processed for RT-PCR. All cultures were carried out at 39°C in an atmosphere of 5% CO_2, 10% O_2, and 85% N_2.

Fixation and Staining of Oocytes for Determination of Nuclear Maturation

At the end of the 44-h IVM culture period, the cumulus investment was removed by hyaluronidase treatment (247 turbidity reducing units/ml) for 10 min, followed by 4 min of vortexing and by repeated pipetting with a narrow-bore micropipette. The oocytes were mounted on microscope slides with petroleum jelly stripes, covered with glass, and fixed in ethanol-acetic acid (3:1, v/v) for at least 24 h. Staining was performed with 2% orcein in 50% aqueous-acetic acid and 1% sodium citrate. After careful substitution of dye with 40% acetic acid, the samples were observed with a phase-contrast NU Zeiss-Jena microscope (Carl Zeiss, Oberkochen, Germany) and examined for stage of nuclear maturation: GV, early diakinesis (ED), late diakinesis (LD), metaphase I (MI), and metaphase II (MII) [34].

Processing of Oocytes for Light-Microscopical Autoradiography and TEM

For autoradiography, COCs directly isolated from small, medium-small, medium-large, and large follicles (nontreated oocytes) were incubated for 20 min in gas-equilibrated BM-PVA supplemented with 100 μCi/ml of [^{3}H]uridine (specific activity, 40 MBq/mM; Amersham, Little Chalfont, UK). After incubation with the precursor, the oocytes were repeatedly washed in prewarmed PBS. The same procedure was performed with COCs from small, medium-small, and large follicles harvested from BL-I culture (BL-I-treated oocytes) in MIM at 4 and 24 h.

After labeling of newly synthesized RNA, the oocytes were fixed in a mixture of 2.5% glutaraldehyde and 2% paraformaldehyde in 0.1 M cacodylate buffer (pH 7.2). Subsequently, the specimens were washed in buffer, postfixed in 1% OsO_4 in 0.1 M cacodylate buffer, embedded in Epon, (Merck, Darmstadt, Germany), and serially sectioned into semithin sections (thickness, 2 μm). Every second section was stained with basic to-

luidine blue and evaluated by bright-field light microscopy. Selected semithin sections were re-embedded as described by Hyttel and Madsen [35] and processed for ultrathin sectioning (thickness, 70 nm). The ultrathin sections were examined using a Philips CM100 transmission-electron microscope (Philips, Eindhoven, The Netherlands).

Neighboring unstained semithin sections were processed for autoradiography for detection of total RNA synthesis and nucleolus-associated RNA synthesis. The sections were coated with Ilford K5 liquid nuclear emulsion (Ilford; Basildon, Essex, UK) and exposed for 6 wk at 4°C. Finally, the specimens were developed in Kodak D19 (Kodak, Rochester, NY) at 17°C, stained with basic toluidine blue, and evaluated by bright-field and epipolarized light microscopy.

Whole-Mount Immunolabeling of Oocytes

Antibodies. The following primary antibodies were employed: human anti-UBF (kindly provided by Dr. Renate Voigt and Dr. Ingrid Grummt, German Cancer Research Center, Heidelberg, Germany) [36], rabbit polyclonal antibody against PAF53 (an RNA Pol I-associated factor; kindly provided by Dr. Lawrence Rothblum, Weis Center for Research, Geisinger Clinic, Pennsylvania, PA) [14], mouse monoclonal anti-p130 (DCS 211.6; kindly provided by Dr. Klaus Hansen, Danish Cancer Society, Copenhagen, Denmark) [37], and mouse monoclonal anti-pRb (Rb 4H1; Cell Signaling Technology, Beverly, MA).

Immunofluorescence. The COCs from small, medium-small, medium-large, and large follicles were denuded by mechanical pipetting, followed by removal of the zona pellucida by 0.5% pronase and fixation in 4% paraformaldehyde PBS immediately on isolation from the follicles. The fixed oocytes were permeabilized for 1 h in PBS containing 1% Triton-X at room temperature, and unspecific antibody binding was blocked for 2 h in PBS supplemented with 5% inactivated goat serum (blocking buffer). Oocytes were subsequently incubated overnight at 4°C with the primary antibodies diluted in blocking buffer. The following day, excess primary antibodies were removed by extensive washing in PBS supplemented with 0.1% Triton X-100 and 3 mg/ml of BSA (washing buffer). Subsequently, oocytes were incubated for 2 h at room temperature with fluorescein isothiocyanate (FITC)-conjugated goat anti-mouse (Jackson ImmunoResearch Laboratories, West Grove, PA), Texas red (TxR)-conjugated goat anti-rabbit, or Cy-5 conjugated donkey anti-human (Jackson ImmunoResearch Laboratories) antibody diluted in blocking buffer, followed by extensive washing. The immunolabeled oocytes were mounted in Vectashield (Vector Laboratories, Burlingame, CA) containing 1 μg/ml of Hoechst 33258 and covered with a coverslip that was fixed to the slide with nail varnish and stored at 4°C in the dark. Control immunostaining of unspecific labeling by the secondary antibody was performed by omitting the primary antibodies (data not shown).

Microscopy and image processing. Immunolabeled oocytes were analyzed by a confocal laser-scanning microscopy (TCS SP2; Leica Microsystems, Wetzlar, Germany). The fluorochromes were excited using the appropriate combination of excitation and barrier filters and argon laser lines for FITC (488 nm) and helium/neon lines for TxR (543 nm) and Cy5 (633 nm).

RNA Isolation and RT-PCR

The COCs from small and large follicles were denuded by repeated pipetting with a narrow-bore micropipette immediately after isolation, washed three times in PBS containing 0.1% PVA, and stored individually at −80°C in a minimum volume (≤5 μl) of medium until experimental use. The same procedure was performed with COCs from small and large follicles harvested from BL-I culture (BL-I-treated oocytes) in MM at 24 h.

Before RNA isolation, 1 pg of rabbit globin RNA (Gibco, Invitrogen, Carlsbad, CA) was added to the samples as an internal standard. Subsequently, Poly(A)$^+$ RNA was isolated from single oocytes with the aid of Dynabeads (Dynal Biotech, Oslo, Norway), as described previously [38], and used immediately for RT, which was carried out in a total volume of 20 μl using 2.5 μM random hexamers (Perkin-Elmer, Vaterstetten, Germany) to get the widest array of cDNA. The RT reaction mixture consisted of 1× RT buffer (50 mM KCl, 10 mM Tris-HCl, pH 8.3), 5 mM $MgCl_2$, 1 mM of each dNTP, 20 IU of RNase inhibitor (Perkin-Elmer), and 50 IU of MuLV reverse transcriptase (Perkin-Elmer). The RT reaction was carried out at 25°C for 10 min, 42°C for 1 h, and then a denaturation step at 99°C for 5 min and flash cooling on ice.

The PCR primers were designed from the coding regions of each gene sequence using the Primer 3 software (http://broad.mit.edu/cgi-bin/primer/primer3_www.cgi). For each pair of gene-specific primers, semilog plots of the fragment intensity as a function of cycle number were used to determine the range of cycle number over which linear amplification occurred, and the number of PCR cycles was kept within this range [38]. Because the total efficiency of amplification for each set of primers during each cycle is not known, such an assay can only be used to compare relative abundances of one mRNA among different samples [39].

The PCR reaction was performed with a gene-specific cDNA oocyte equivalent and 50 fg of globin RNA in a final volume of 50 μl of 1× PCR buffer (20 mM Tris-HCl [pH 8.4], 50 mM KCl), 1.5 mM $MgCl_2$, 200 μM of each dNTP, 1 μM of each sequence specific primer, and 0.5 μM of each globin primer using a PTC-200 thermocycler (MJ Research, Waltham, MA). To ensure specific amplification, a ''hot-start'' PCR was employed by adding 1 IU of Taq DNA polymerase (Gibco) at 72°C.

The PCR program employed an initial step of 97°C for 2 min and 72°C for 2 min (hot start), followed by different cycle numbers of 15 sec each at 95°C for DNA denaturation, 15 or 25 sec at different temperatures for annealing of primers, and 15 sec at 72°C for primer extension. The last cycle was followed by a 5-min extension at 72°C and cooling to 4°C. As negative controls, tubes were prepared in which RNA or reverse transcriptase were omitted during the RT reaction (data not shown). The sequences of the primers used, the annealing temperatures, the gene-specific oocyte equivalents, and the fragment sizes are summarized in Table 1.

The RT-PCR products were subjected to electrophoresis on a 2% agarose gel in 1× TBE buffer (90 mM Tris, 90 mM borate, 2 mM EDTA, pH 8.3) containing 0.2 μg/ml of ethidium bromide. Additional ethidium bromide at the same concentration was added to the running buffer. The image of each gel was recorded using a CCD camera (Quantix; Photometrics, München, Germany) and the IPLab Spectrum program (Scanalytics, Fairfax, VA). The intensity of each band was assessed by densitometry using an image-analysis program (IPLab Gel; Scanalytics). The relative amount of the mRNA of interest was calculated by dividing the intensity of the band for each developmental stage by the intensity of the globin band for the corresponding stage. Experiments were repeated with at least eight oocytes for each mRNA.

The general RNA recovery rate was estimated as the ratio between the intensity of the globin band with and without RNA preparation procedure, starting with an equivalent of 50 fg of globin in the PCR reaction. On average, 46% of poly(A)$^+$-tailed RNA was recovered using our Dynabeads oligo-d(T) mRNA isolation method, which corresponds well with other published yields [40].

The number of replicates was calculated to get an acceptable repeatability of the assay (0.90). The average repeatability (precision) of the assay varied from 0.60 to 0.70. Therefore, a minimum of 10 replicates had to be performed.

Statistical Analysis

The effects of the different treatments within each individual maturation group were analyzed by the Fisher exact test using pairwise compar-

TABLE 1. Primers used for PCR.

Genes	5′ Primer sequence	3′ Primer sequence	T_{ann} (°C)[b]/cycle number	Oocyte equivalent	Fragment size (base pairs)
Globin	GCAGCCACGGTGGCGAGTAT	GTGGGACAGGAGCTTGAAAT	60/27	0.05	257
PAF53[a]	GAGGGTGTCCAGAAACCAGA	TGATGCCATCCACAGTGATT	60/33	1.0	292
UBF[a]	CGAAGACCAAAAGCGATACGAGAG	TATGCTGCACGTTCCTGGGGAGACA	60/34	0.4	330
p130[a]	CCACCTTGTGTTATTGAGAAACTCT	CTCATAGGCTTTATTGATGGCTTTA	57/36	0.5	204
RB[a]	CTTCGGATTTGAGCATGGAT	TGGAAATGCAGAGAACACCA	57/36	4.0	302

[a] The primer pair to detect these mRNAs was first designed from the given homologue sequence, and the product was sequenced. The resulting ''porcine-specific'' sequence was used to create the primer pair employed to detect the transcript of interest.
[b] T_{ann}, annealing temperature.

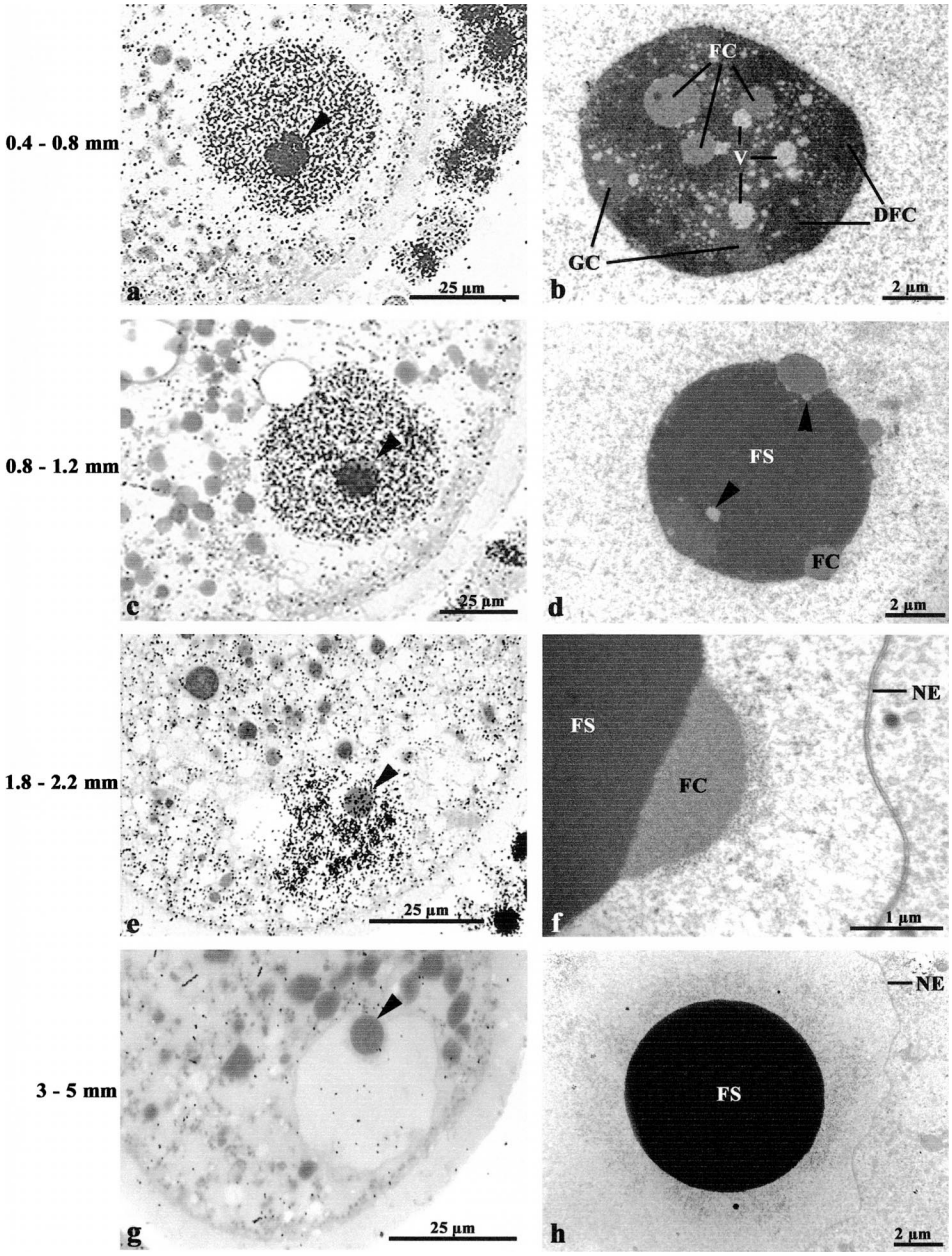

FIG. 2. Light-microscopical autoradiographs (**a**, **c**, **e**, and **g**) and electron micrographs (**b**, **d**, **f**, and **h**) of nontreated oocytes from small (diameter, 0.4–0.8 mm; **a** and **b**), medium-small (diameter, 0.8–1.2 mm; **c** and **d**), medium-large (diameter, 1.8–2.2 mm; **e** and **f**), and large (diameter, 3–5 mm; **g** and **h**) follicles. Note the intense autoradiographic labeling over the nucleolus (arrowheads) in oocytes from small follicles, which decrease with the increase in follicle size (**a**, **c**, **e**, and **g**). The electron micrographs show in detail the nucleoli from all size categories. Oocyte nucleoli from small follicles display several fibrillar centers (FC) surrounded by vacuoles (V), dense fibrillar component (DFC), and granular component (GC; **b**). In medium-small oocytes, the nucleoli have compacted to fibrillar spheres (FS), in the periphery of which the FCs are partially embedded, often surrounded by small vacuoles (arrowheads; **d**). In nucleoli from medium-large oocytes, the FCs are further marginalized to cap-like structures on the surface of the FSs, and in oocytes from large follicles, the FSs are more or less devoid of fibrillar centers (**f** and **h**). NE, nuclear envelope.

isons. Differences of $P < 0.05$ were considered to be significant. The software program GraphPad InStat (Version 3.00 for Windows NT; GraphPad Software, San Diego, CA) was used for the statistical calculations.

Relative abundances in the RT-PCR experiments were analyzed using the SigmaStat 2.0 (Jandel Scientific, San Rafael, CA) software package. After testing for normality (Kolmogorov-Smirnov test with Lilliefor correction) and testing for equal variance (Levene median test), an ANOVA followed by multiple pairwise comparisons using the Tukey test was employed. Differences of $P < 0.05$ were considered to be significant.

RESULTS

Autoradiography and Ultrastructure

In oocytes of all follicle sizes, the nuclei were located peripherally except for a few oocytes from small follicles, in which they were located more centrally.

Nontreated oocytes. Nontreated oocytes from small follicles (diameter, 0.4–0.8 mm; n = 5) displayed intensive autoradiographic labeling over nucleoplasm and nucleoli (Fig. 2a). The nucleoli were spherical and fibrillogranular, and they contained several FCs and vacuoles embedded in a DFC and a GC (Fig. 2b).

The nuclei in oocytes from medium-small follicles (diameter, 0.8–1.2 mm; n = 5) displayed intensive autoradiographic labeling over the nucleoplasm, whereas the nucleoli were only partially labeled (Fig. 2c). The nucleoli appeared as compacted spheres of densely packed fibrils, in the periphery of which the FCs were partially embedded and often surrounded by small vacuoles (Fig. 2d).

The nuclei in oocytes from medium-large follicles (diameter, 1.8–2.2 mm; n = 5) displayed decreased autoradiographic labeling over both nucleoplasm and nucleoli (Fig. 2e). Moreover, the FCs were observed as cap-like structures on the surface of the compact fibrillar spheres (Fig. 2f).

The nuclei in oocytes from large follicles (diameter, 3–6 mm; n = 5) did not display autoradiographic labeling (Fig. 2g). The nucleoli had developed into compact fibrillar spheres more or less devoid of FCs (Fig. 2h).

BL-I-treated oocytes. In BL-I treated oocytes, cumulus expansion did not occur, and in particular, after 24 h of

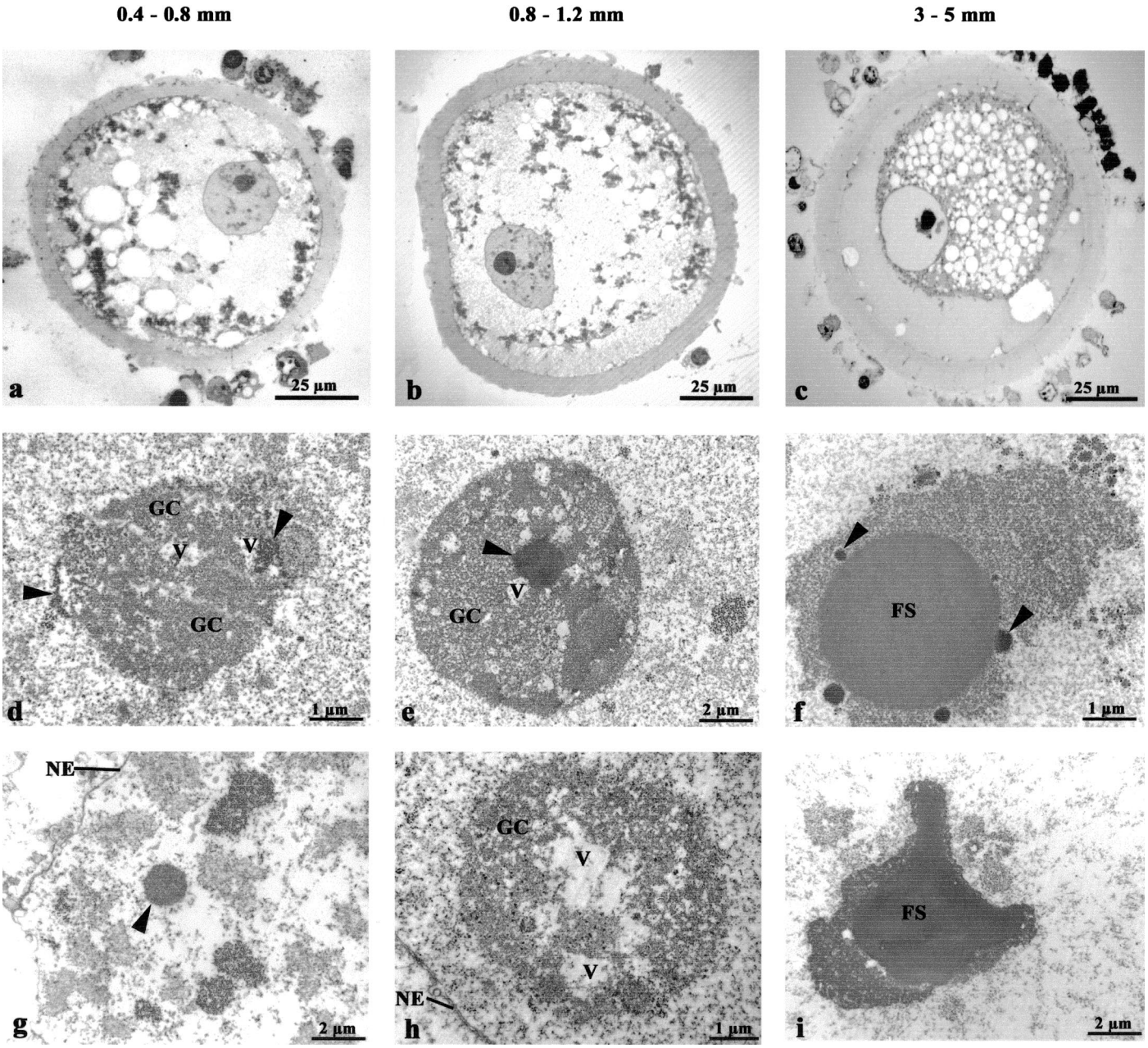

FIG. 3. Light-microscopical autoradiographs (**a**–**c**) and electron micrographs (**d**–**i**) of oocytes from small (diameter, 0.4–0.8 mm; **a**, **d**, and **g**), medium-small (diameter, 0.8–1.2 mm; **b**, **e**, and **h**), and large (diameter, 3–5 mm; **c**, **f**, and **i**) follicles treated with 100 µM BL-I for 4 h (**a**–**f**) and 24 h (**g**–**i**). The electron micrographs show in detail the nucleoli from all size categories. In oocytes from small follicles after 4 h of treatment with BL-I, the nucleoli present several more or less irregular vacuoles (V) and a granular component (GC), whereas the fibrillar components are condensed to electron-dense structures (arrowheads; **d**). After 24 h, the nucleoli are completely disintegrated, and larger areas of different electron density (arrowheads) are scattered in the nucleoplasm (**g**). In oocytes from medium-small follicles, the nucleoli by and large resemble those of the oocytes from small follicles after 4 h of treatment (**e**), and this nucleolus morphology is more or less maintained until 24 h of culture (**h**). Nucleoli from medium-large follicles are compacted to electron-dense fibrillar spheres (FS) after 4 h, with condensed electron-dense fibrillar centers (arrowheads) on the surface (**f**). After 24 h, the nucleoli display a central sphere of densely packed fibrils (FS) surrounded by electron-dense material (**i**). NE, nuclear envelope.

culture with BL-I, pronounced undulation of the nuclear envelope was observed (Fig. 3, a–c). None of the oocytes (n = 60) showed autoradiographic labeling after 4 h (data not shown) or 24 h (data not shown) of incubation with 100 µM BL-I. Moreover, the ultrastructure of the nucleoli differed significantly from that observed in the nontreated oocytes.

In oocytes from small follicles treated for 4 h with BL-I (n = 8), the nucleoli were spherical and presented several more or less irregular vacuoles of varying sizes (Fig. 3d). The GC of the nucleoli could still be detected, whereas the fibrillar portions (DFC and FCs) apparently had condensed to electron-dense structures. After 24 h (n = 8) of incubation, the nucleoli had completely disintegrated, and structures of varying electron-density were scattered around in the nucleoplasm (Fig. 3g).

In oocytes from medium-small follicles treated for 4 h with BL-I (n = 8), the nucleoli by and large resembled those of the oocytes from small follicles (Fig. 3e). However, in contrast to small follicles, the oocytes from medium-small follicles maintained this nucleolus morphology even after 24 h (n = 10) of culture (Fig. 3h).

TABLE 2. Progression of meiosis in growing and fully grown porcine oocytes after 44-h IVM culture with (BL-1) or without (control) 24-h previous incubation in BL-1.

Follicle diameter (mm)	Total number of oocytes	GV (n [%])	ED (n [%])	LD (n [%])	MI (n [%])	MII (n [%])
Control, small (0.4–0.8)	19	7 (37)	11 (58)[a]	1 (5)	0 (0)	0 (0)
BL-1, small (0.4–0.8)	21	21 (100)	0 (0)[b]	0 (0)	0 (0)	0 (0)
Control, medium-small (0.8–1.2)	22	3 (14)	0 (0)[a]	19 (86)[a]	0 (0)	0 (0)
BL-1, medium-small (0.8–1.2)	37	6 (16)	20 (54)[b]	11 (30)[b]	0 (0)	0 (0)
Control, large (3–5)	20	2 (10)	0 (0)	0 (0)[a]	0 (0)	18 (90)[a]
BL-1, large (3–5)	54	10 (19)	7 (13)	35 (65)[b]	2 (4)	0 (0)[b]

[a,b] Figures with different superscript letters within columns are significantly different ($P < 0.0001$).

In oocytes from large follicles treated for 4 h with BL-I (n = 10), the nucleoli appeared as compact, electron-dense fibrillar spheres (Fig. 3f). Condensed electron-dense FCs were located on the surface. However, the nucleoli in 3 of 10 oocytes were disintegrated after 24 h of culture. The remaining seven oocytes displayed nucleoli composed of a central sphere of densely packed fibrils surrounded by electron-dense material (Fig. 3i).

Reversibility of BL-I-Induced Arrest

To study the reversibility of BL-I-induced arrest, oocytes from small, medium-small, and large follicles were cultured for 24 h in MIM, followed by 44 h of maturation in normal MM. As a control, oocytes from the same follicle size categories were directly submitted to 44-h IVM culture. In oocytes from small follicles, a significant number of control oocytes had progressed into ED compared to the BL-I-treated oocytes (Table 2). Both control and BL-1-treated oocytes from medium-small follicles had entered diakinesis. However, 86% of the control oocytes were in LD, whereas only 29% BL-I-treated oocytes had entered this developmental stage. The majority (90%) of the control oocytes from large follicles had progressed to MII, whereas none of the corresponding BL-I-inhibited oocytes had reached MII.

Whole-Mount Immunolabeling of Oocytes

Localization of p130, UBF, and PAF53 (the associated factor of RNA Pol I) to the nuclei of oocytes in all size categories was investigated by immunocytochemistry. In general, p130 localization was characterized by a diffuse pattern, whereas PAF53 and UBF were localized to foci of different sizes that were either scattered or clustered. Moreover, UBF and PAF53 were colocalized in all size categories, whereas pRb was immunocytochemically undetectable in all size categories. Localization of labeling is referred to as nucleolar (in the presumptive nucleolus) or nucleoplasmic (outside the nucleolus in the surrounding nucleoplasm). These results are summarized in Table 3 and illustrated in Figure 4.

In oocytes from small follicles, UBF (n = 55) and PAF53 (n = 25) were colocalized to deeply located nucleolar foci of different sizes and of varying numbers (Fig. 4, a and e). However, the pocket protein p130 (n = 30) was exclusively localized to the nucleoplasm (Fig. 4i).

In oocytes from medium-small follicles, UBF (n = 65) and PAF53 (n = 20) were predominantly located to large nucleolar foci (Fig. 4, b and f). The p130 (n = 35) was predominantly localized to the nucleolus, where it became colocalized with UBF, at least in the periphery of the UBF foci (Fig. 4j).

In oocytes from medium-large follicles, UBF (n = 40) and PAF53 (n = 20) were observed at foci toward the nucleolar periphery, and the number of foci had decreased (Fig. 4, c and g). The p130 (n = 20) was again predominantly localized to the nucleoplasm (Fig. 4k). However, some colocalization with UBF in the periphery of the foci could still be observed.

In oocytes from large follicles, UBF (n = 50) and PAF53 (n = 20) were colocalized to a few peripheral nucleolar foci and to small nucleoplasmic foci (Fig. 4, d and h). Moreover, PAF53 was undetectable in 25% of the analyzed oocytes. The p130 (n = 30) was exclusively localized to the nucleoplasm, as in oocytes from small follicles (Fig. 4l).

mRNA Expression of Nucleolar-Related Proteins

To analyze whether the proteins involved in rRNA synthesis were regulated at the mRNA level during oocyte growth, we examined the relative abundance of gene transcripts by a semiquantitative RT-PCR assay in oocytes from

TABLE 3. Patterns of nucleolar protein localization in oocytes from different follicle size categories.[a]

Nucleolar protein	Labeling pattern	Follicle size category			
		Small	Medium-small	Medium-large	Large
UBF	n	55 (100)	65 (100)	40 (100)	50 (100)
	Deep nucleolar foci	55/55 (100)	65/65 (100)	10/40 (25)	2/50 (4)
	Peripheral nucleolar foci	2/55 (3.6)	6/65 (9.2)	33/40 (83)	50/50 (100)
	Nucleoplasmic foci	15/55 (27.3)	11/65 (16.9)	11/40 (27.5)	5/30 (16.7)
PAF53	n	25 (100)	20 (100)	20 (100)	20 (100)
	Deep nucleolar foci	25/25 (100)	14/20 (70)	4/20 (20)	1/20 (5)
	Peripheral nucleolar foci	4/25 (16)	3/20 (15)	16/20 (80)	20/20 (100)
	Nucleoplasmic foci	8/25 (32)	4/20 (20)	1/20 (5)	0/20 (0)
	Undetectable				5/20 (25)
p130	n	30 (100)	35 (100)	20 (100)	30 (100)
	Diffuse nucleolar	0/30 (0)	32/35 (91)	4/20 (20)	0/30 (0)
	Diffuse nucleoplasmic	30/30 (0)	16/35 (46)	20/20 (100)	30/30 (100)

[a] No. of labeled oocytes/no. of oocytes examined (% labeled).

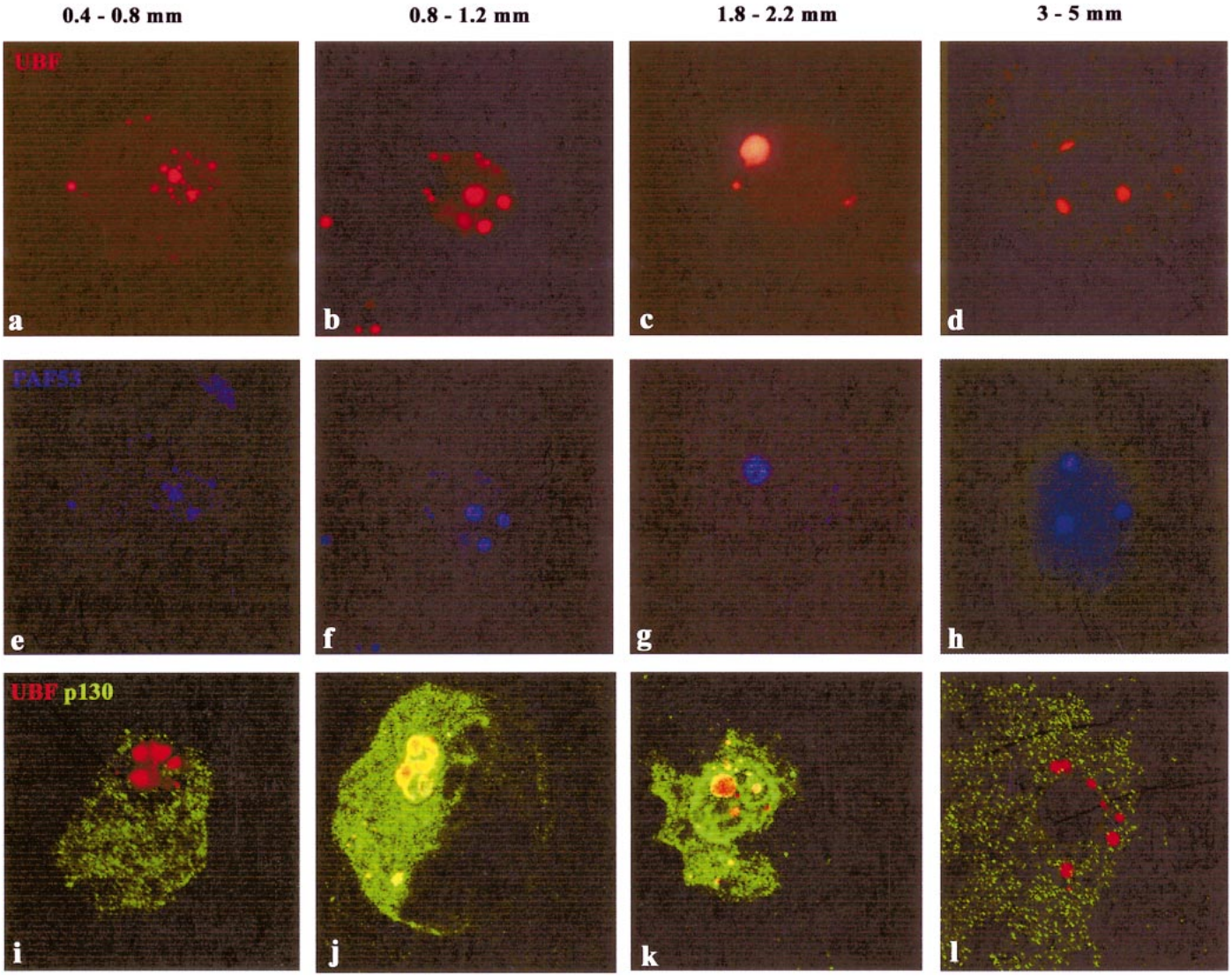

FIG. 4. Confocal laser-scanning micrographs of porcine oocyte nuclei from small (diameter, 0.4–0.8 mm; **a**, **e**, and **i**), medium-small (diameter, 0.8–1.2 mm; **b**, **f**, and **j**), medium-large (diameter, 1.8–2.2; **c**, **g**, and **k**), and large (diameter, 3–5 mm; **d**, **h**, and **l**) follicles immunolabeled with antibodies against nucleolar proteins UBF (**a**–**d**), PAF53 (**e**–**h**), and UBF/p130 (**i**–**l**; UBF, red; p130, green; colocalization, yellow). The intensity of the fluorescent signals does not express the abundance of the proteins. Note that UBF and p130 are colocalized in oocytes from medium-small follicles and, to some degree, medium-large follicles. The first two rows display the same oocytes immunostained with UBF (first row) and PAF53 (lower row). The last row displays different oocytes coimmunostained with UBF and p130.

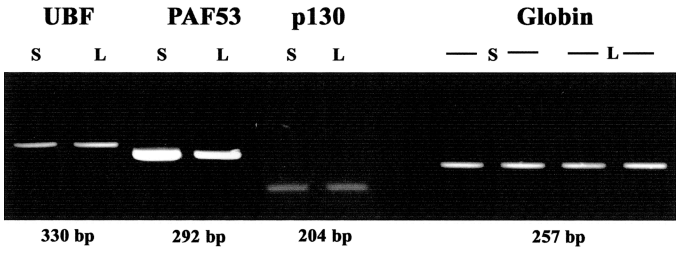

FIG. 5. Representative gel photograph of a semiquantitative RT-PCR analysis of genes involved in rRNA synthesis: UBF, PAF53, and p130. The internal standard, globin, is shown next to these genes. Each lane represents the RT-PCR product derived from polyA$^+$ RNA from the oocyte equivalents listed in Table 1. For each gene, the RT-PCR product is shown in oocytes from small (S) and large (L) follicles.

small (n = 80) and large (n = 80) follicles. The mean value, from 8 to 12 replicates, of the relative abundance of gene transcripts was calculated. A representative gel photo of the mRNA expression of UBF, PAF53, and p130 is shown in Figure 5.

Nontreated oocytes. The relative abundance of UBF mRNA was unaffected during oocyte growth (0.4 ± 0.09 [mean ± SEM] in oocytes from small follicles and 0.4 ± 0.15 in oocytes from large follicles). However, the relative abundance of PAF53 was significantly decreased (P = 0.013) from 3.0 ± 0.42 (small follicles) to 1.5 ± 0.37 (large follicles).

The relative abundance of p130 mRNA was similarly low in oocytes from small (0.19 ± 0.05) and large (0.14 ± 0.04) follicles. The mRNA expression of the other pocket protein, pRb, was also examined, but it was undetectable in RNA isolated from one oocyte equivalent. In pools of five oocytes, the relative abundance of pRb expression was

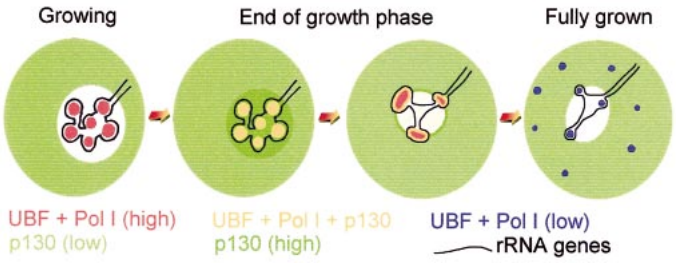

FIG. 6. Model for down-regulation of rRNA gene transcription at the end of the oocyte growth phase. Each drawing represents an oocyte nucleus. During oocyte growth, UBF and PAF53 are fully colocalized, as illustrated in red (high RNA Pol I) and blue (low RNA Pol I). In growing oocytes, UBF and PAF53 are localized to numerous fibrillar centers in the nucleolus, where rRNA synthesis occurs. The p130 is exclusively localized to the nucleoplasm (light green). In oocytes approaching the end of growth phase, p130 is targeted to the nucleolus (dark green), where it becomes colocalized (yellow), especially at the periphery of the fibrillar centers, with and inactivates UBF. Concomitantly, the transcription of PAF53 is downregulated. In fully grown oocytes, p130 reassumes a nucleoplasmic localization and is excluded from the nucleolus. The UBF is still localized to the fibrillar centers at the periphery of the nucleolus but no longer needs to be inactivated by p130, because the cellular content of PAF53 is significantly reduced. The rRNA genes are shown in dark blue.

detectable, and no significant difference was observed between oocytes from small (3.2) and large (2.3) follicles.

BL-I-treated oocytes. We were unable to detect mRNA of UBF in oocytes from either small (n = 10) or large (n = 10) follicles that had been treated with 100 μM BL-I for 24 h. Similarly, the relative abundance of PAF53 mRNA was significantly decreased in oocytes from small (n = 10; from 3.0 ± 0.42 to 0.80 ± 0.09; $P = 0.001$) and large follicles (n = 10; from 1.5 ± 0.37 to 0.39 ± 0.09; $P = 0.027$) when treated with BL-I. Moreover, as in nontreated oocytes, the relative abundance in oocytes from small follicles was significantly higher ($P = 0.009$) compared to oocytes from large follicles. Finally, the relative abundance of p130 in oocytes from small (n = 6; 0.29 ± 0.2) and large oocytes (n = 6; 0.28 ± 0.2) was comparable to the levels found in nontreated oocytes.

DISCUSSION

Results of the present study revealed, to our knowledge for the first time, insight regarding the complex and well-orchestrated pattern of rRNA transcription and processing in porcine oocytes at different stages of follicular development. The activity of RNA synthesis decreases gradually as the oocyte reaches full size and becomes meiotically competent. Concomitantly, the oocyte nucleolus changes from being fibrillogranular, with several FCs and vacuoles embedded in a DFC and a GC, to becoming less vacuolated, with marginalized FCs and compaction of the remaining portions to a sphere of densely packed fibrils without recognizable nucleolar ultrastructure.

During oocyte growth, UBF and the RNA Pol I-associated factor PAF53 were colocalized and displayed nucleolar localization. In growing oocytes, UBF and PAF53 were concentrated in foci localized deeply in the nucleolar compartment, and with the completion of growth, these foci moved toward the nucleolar periphery. According to previous localization of UBF and RNA Pol I to the FCs of the nucleolus [41–43], the labeled foci probably represent FCs, in accordance with the ultrastructural demonstration of the peripheral movement of these structures.

The so-called pocket proteins pRb and p130 are potent suppressors of cell growth and proliferation that act by modulating transcription [24, 25]. It was discovered that pRb represses transcription of the rRNA genes, presumably by inactivating RNA Pol I [44]. Later, it was found that both p130 and pRb more specifically inhibit rRNA gene transcription by preventing UBF from interacting with the selectivity factor SL-1, which in turn blocks the formation of the transcription initiation complex [26–29]. In agreement with this observation, accumulation of pRb in the nucleoli of confluent fibroblasts correlates with a decrease in rRNA synthesis [27]. Moreover, p130 and pRb display functional overlap in downregulating rRNA synthesis in somatic cells, because the RNA Pol I transcription was unaffected in pRb-knockout fibroblasts but was abnormally elevated in pRb/p130 double-knockout fibroblasts [26].

Our data suggest that p130, but not pRb, is involved in downregulation of rRNA synthesis at the end of oocyte growth. In growing porcine oocytes, p130 was exclusively located in the nucleoplasm. However, at the end of the growth phase, double-immunostaining of UBF and p130 revealed structural colocalization of the proteins, because p130 was found at the periphery of the nucleolar UBF foci. This colocalization likely is causally involved in the downregulation of rRNA synthesis at the end of oocyte growth.

On cell-cycle arrest in somatic cells, the decrease in rRNA synthesis correlates with a decrease in the cellular content of PAF53, whereas the cellular content of UBF does not change [27]. Therefore, we analyzed the mRNA expression of PAF53 and UBF during the growth of porcine oocytes by semiquantitative RT-PCR. Our data show that the mRNA and protein levels of UBF remained unchanged during growth of porcine oocytes. However, the mRNA expression of PAF53 was significantly decreased, an effect that may also be detectable at the protein level, because PAF53 could not be detected in 25% of the fully grown oocytes. These data also indicate that the downregulation of PAF53 may play an important role during inactivation of rRNA synthesis at the end of oocyte growth.

Despite differences in the ultrastructure of nucleoli in GV oocytes compared to nucleoli of cycling somatic cells, the molecular organization of the rRNA synthesis and processing machinery are apparently comparable. In mouse oocytes, downregulation of rRNA gene transcription at the end of oocyte growth is not associated with physical detachment of the RNA Pol I transcription complex from its binding site at the nucleolus organizer regions but, rather, is caused by regulation of the activity of proteins (e.g., UBF) involved in forming the transcription initiation complex [45].

Based on the present data, we propose the following model for downregulation of rRNA gene transcription at the end of the porcine oocyte growth phase (Fig. 6). In growing oocytes, UBF and the RNA Pol I-associated factor, PAF53, are localized to numerous FCs in the nucleolus, where rRNA synthesis occurs. The p130 is exclusively localized to the nucleoplasm. In oocytes approaching the end of the growth phase, p130 is targeted to the nucleolus, where it becomes colocalized with and inactivates UBF and, thus, rRNA synthesis. Concomitantly, transcription of PAF53 is downregulated. Subsequently, the FCs become fewer, larger, and finally, marginalized. Partial colocalization of UBF and p130 may still be seen. In fully grown oocytes, p130 reassumes a nucleoplasmic localization and is excluded from the nucleolus. The UBF is still localized to the FCs on the periphery of the nucleolus. However, it no longer needs to be inactivated by p130, because the

cellular content of messengers encoding PAF53 is significantly reduced. Finally, the FCs may form fragments that spread in the nucleoplasm.

Various agents, such as BL-I and roscovitine, have been shown to inhibit GVBD in bovine [31, 46, 47] and porcine oocytes [48, 49]. In bovine oocytes, 24 h of incubation with 100 μM BL-I was reversible; 95% of the blocked oocytes were able to resume meiosis and progress to MII after removal of the drug [32, 50]. In porcine oocytes, one study showed that 24-h inhibition with 100 μM BL-I resulted in a reduced rate (25%) of oocytes, which were subsequently able to mature to MII [51]. However, another study, which only analyzed the reversibility of 12.5 μM BL-I, showed that oocytes inhibited for 20 h with 12.5 μM BL-I, followed by 24 h of normal IVM, reached MII at levels similar to those of untreated oocytes [33]. Because this latter study was reported after the initiation of our experiments, we employed a concentration of 100 μM BL-I for inhibition in prolongation of previous experiments in our laboratory [51].

Our data show that 24-h incubation with 100 μM BL-I has a detrimental effect on GVBD during subsequent IVM of porcine oocytes regardless of whether they were growing or had completed their growth phase. These data support the notion that porcine oocytes are more sensitive than bovine oocytes to BL-I. Moreover, we found that BL-I severely affected the ultrastructure of the oocyte nucleoli. The changes of the nucleolar ultrastructure very likely inhibited the rRNA synthetic capability, because the fibrillar components, where rRNA transcription and initial processing occur, condensed to electron-dense, inactive structures or even disintegrated. The RT-PCR data further support the severe effect of BL-I, because mRNA expression of UBF was undetectable in treated oocytes. Likewise, the mRNA expression of PAF53 was significantly reduced in BL-I-treated oocytes compared to nontreated oocytes. However, as in nontreated oocytes, the PAF53 mRNA expression in BL-1-treated specimens was still higher in growing than in fully grown oocytes. Moreover, the p130 mRNA expression in BL-1-treated oocytes was unaffected by the BL-I treatment. This latter fact indicates that the induced reduction of the messengers encoding PAF53 and UBF is not caused by unspecific RNA degradation but, rather, by specific regulation of gene expression. Finally, it should be stressed that we cannot exclude the idea that the described detrimental effect of BL-I is based on toxic effects resulting from the relatively high concentration (100 μM) employed.

The GVBD of oocytes is accompanied by a major occurrence of protein phosphorylation in several species, including *Xenopus* [52], mice [53], sheep [54], goat [55], and cattle [56]. The cdk1, which is the catalytic subunit of the maturation-promoting factor (MPF), is activated in association with this burst of phosphorylation, and resumption of meiosis is controlled by the MPF complex of cdk1 and cyclin B [57]. Moreover, prevention of GVBD and meiotic cell-cycle arrest induced by BL-I and roscovitine has been shown to be mediated through inhibition of activation of MPF [51, 58]. However, BL-I inhibits not only GVBD but also rRNA synthesis, and this may be through separate mechanisms.

Differential phosphorylation of UBF is emerging as a focal point for cell cycle-dependent oscillations of rRNA synthetic activity. Transcriptional silencing in quiescent or serum-deprived somatic cells correlates with hypophosphorylation of UBF, and phosphorylation of UBF increases in conjunction with the increase in rRNA gene transcription [36, 59, 60]. Moreover, dephosphorylation of UBF completely abolishes binding of UBF to SL-1 and prevents transcriptional activation of rRNA genes [22]. Additionally, the UBF activity is cell-cycle regulated via cdk phosphorylation, and the cdk-mediated phosphorylation of UBF is required for interaction with SL-1 and correlates with activation of rRNA synthesis [23, 61, 62]. Consequently, because BL-1 inhibits cdk, the BL-I-induced inhibition of rRNA synthesis that we observed in the porcine oocytes likely is caused by dephosphorylation and resulting inactivation of UBF. Moreover, the activity of UBF can, as alluded to before, be altered by interaction with other proteins. Data from somatic cells show that hypophosphorylated, active pocket proteins bind to UBF [27]. Because BL-I-induced inhibition of cdk might lead to an increase in hypophosphorylated p130, this likely would lead to an increased association between UBF and p130, thereby preventing UBF from binding to SL-1 to form the transcription initiation complex. Therefore, it would be interesting to analyze the phosphorylation status of UBF and p130 during oocyte growth and the possible interaction between UBF and p130.

In conclusion, the present results indicate that the pocket protein p130 is involved in downregulation of rRNA transcription at the end of oocyte growth via interaction with UBF. Synthesis of rRNA is further regulated by a decrease in the expression of mRNA encoding the RNA Pol I-associated factor PAF53. At the ultrastructural level, these molecular changes are paralleled by marginalization of the FCs of the oocyte nucleolus, followed by compaction to an inactive sphere of fibrils. Additionally, meiotic inhibition by the cdk-inhibitor BL-I, in concentrations that allow for development in cattle, has a detrimental effect on the nucleolus morphology in porcine oocytes as well as on the competence of the gametes to resume meiosis. Moreover, the mRNA expression of UBF and PAF53 was significantly reduced or even absent, whereas the relative abundance of mRNA encoding p130 was unaffected by BL-I inhibition.

ACKNOWLEDGMENTS

The authors are grateful to Ms. Jytte Nielsen and Mr. Vaclav Pech for careful embedding and sectioning of specimens and to Mrs. Patricia Jandurova, Mrs. Lenka Travnickova, and Ms. Katerina Opatova for isolation of the oocytes.

REFERENCES

1. Abeydeera LR. In vitro fertilization and embryo development in pigs. Reprod Suppl 2001; 58:159–173.
2. Niemann H, Rath D. Progress in reproductive biotechnology in swine. Theriogenology 2001; 56:1291–1304.
3. Funahashi H, Day BN. Advances in in vitro production of pig embryos. J Reprod Fertil Suppl 1997; 52:271–283.
4. Parrish JJ, Kim CI, Bae IH. Current concepts of cell-cycle regulation and its relationship to oocyte maturation, fertilization, and embryo development. Theriogenology 1992; 38:227–296.
5. Crozet N, Ahmed-Ali M, Dubos MP. Developmental competence of goat oocytes from follicles of different size categories following maturation, fertilization, and culture in vitro. J Reprod Fertil 1995; 103: 293–298.
6. Cognie Y, Benoit F, Poulin N, Khatir H, Driancourt MA. Effect of follicle size and of the FecB Booroola gene on oocyte function in sheep. J Reprod Fertil 1998; 112:379–386.
7. Pavlok A, Lucas-Hahn A, Niemann H. Fertilization and developmental competence of bovine oocytes derived from different categories of antral follicles. Mol Reprod Dev 1992; 31:63–67.
8. Tsafriri A, Channing CP. Influence of follicular maturation and culture conditions on the meiosis of pig oocytes in vitro. J Reprod Fertil 1975; 43:149–152.

9. Motlik J, Crozet N, Fulka J. Meiotic competence in vitro of pig oocytes isolated from early antral follicles. J Reprod Fertil 1984; 72: 323–328.
10. Crozet N, Motlik J, Szollosi D. Nucleolar fine structure and RNA synthesis in porcine oocytes during early stages of antrum formation. Biol Cell 1981; 41:35–42.
11. Motlik J, Kopecny V, Travnik P, Pivko J. RNA synthesis in pig follicular oocytes. Autoradiographic and cytochemical study. Biol Cell 1984; 50:229–235.
12. Leary DJ, Huang S. Regulation of ribosome biogenesis within the nucleolus. FEBS Lett 2001; 509:145–150.
13. Wachtler F, Stahl A. The nucleolus: a structural and functional interpretation. Micron 1993; 24:473–505.
14. Hannan KM, Hannan RD, Rothblum LI. Transcription by RNA polymerase I. Front Biosci 1998; 3:d376–d398.
15. Grummt I. Regulation of mammalian ribosomal gene transcription by RNA polymerase I. Prog Nucleic Acid Res Mol Biol 1999; 62:109–154.
16. Hanada K, Song CZ, Yamamoto K, Yano K, Maeda Y, Yamaguchi K, Muramatsu M. RNA polymerase I associated factor 53 binds to the nucleolar transcription factor UBF and functions in specific rDNA transcription. EMBO J 1996; 15:2217–2226.
17. Jantzen HM, Chow AM, King DS, Tjian R. Multiple domains of the RNA polymerase I activator hUBF interact with the TATA-binding protein complex hSL1 to mediate transcription. Genes Dev 1992; 6: 1950–1963.
18. Paule MR. Transcription of ribosomal RNA by eukaryotic RNA polymerase I. In: Conaway RC, Conaway JW (eds.), Transcription: Mechanisms and Regulation. New York: Raven Press; 1994: 83–104.
19. Bell SP, Learned RM, Jantzen HM, Tjian R. Functional cooperativity between transcription factors UBF1 and SL1 mediates human ribosomal RNA synthesis. Science 1988; 241:1192–1197.
20. Comai L, Tanese N, Tjian R. The TATA-binding protein and associated factors are integral components of the RNA polymerase I transcription factor, SL1. Cell 1992; 68:965–976.
21. Learned RM, Learned TK, Haltiner MM, Tjian RT. Human rRNA transcription is modulated by the coordinate binding of two factors to an upstream control element. Cell 1986; 45:847–857.
22. Tuan JC, Zhai W, Comai L. Recruitment of TATA-binding protein-TAFI complex SL1 to the human ribosomal DNA promoter is mediated by the carboxy-terminal activation domain of upstream binding factor (UBF) and is regulated by UBF phosphorylation. Mol Cell Biol 1999; 19:2872–2879.
23. Voit R, Grummt I. Phosphorylation of UBF at serine 388 is required for interaction with RNA polymerase I and activation of rDNA transcription. Proc Natl Acad Sci U S A 2001; 98:13631–13636.
24. Grana X, Garriga J, Mayol X. Role of the retinoblastoma protein family, pRB, p107, and p130, in the negative control of cell growth. Oncogene 1998; 17:3365–3383.
25. Tonini T, Hillson C, Claudio PP. Interview with the retinoblastoma family members: do they help each other? J Cell Physiol 2002; 192: 138–150.
26. Ciarmatori S, Scott PH, Sutcliffe JE, McLees A, Alzuherri HM, Dannenberg JH, te Riele H, Grummt I, Voit R, White RJ. Overlapping functions of the pRb family in the regulation of rRNA synthesis. Mol Cell Biol 2001; 21:5806–5814.
27. Hannan KM, Kennedy BK, Cavanaugh AH, Hannan RD, Hirschler-Laszkiewicz I, Jefferson LS, Rothblum LI. RNA polymerase I transcription in confluent cells: Rb down-regulates rDNA transcription during confluence-induced cell cycle arrest. Oncogene 2000; 19:3487–3497.
28. Hannan KM, Hannan RD, Smith SD, Jefferson LS, Lun M, Rothblum LI. Rb and p130 regulate RNA polymerase I transcription: Rb disrupts the interaction between UBF and SL-1. Oncogene 2000; 19:4988–4999.
29. Voit R, Schafer K, Grummt I. Mechanism of repression of RNA polymerase I transcription by the retinoblastoma protein. Mol Cell Biol 1997; 17:4230–4237.
30. Lonergan P, Faerge I, Hyttel PM, Boland M, Fair T. Ultrastructural modifications in bovine oocytes maintained in meiotic arrest in vitro using roscovitine or butyrolactone. Mol Reprod Dev 2003; 64:369–378.
31. Mermillod P, Tomanek M, Marchal R, Meijer L. High developmental competence of cattle oocytes maintained at the germinal vesicle stage for 24 hours in culture by specific inhibition of MPF kinase activity. Mol Reprod Dev 2000; 55:89–95.
32. Pavlok A, Kanka J, Motlik J, Vodicka P. Culture of bovine oocytes from small antral follicles in meiosis-inhibiting medium with butyrolactone I: RNA synthesis, nucleolar morphology and meiotic competence. Anim Reprod Sci 2000; 64:1–11.
33. Wu GM, Sun QY, Mao J, Lai L, McCauley TC, Park KW, Prather RS, Didion BA, Day BN. High developmental competence of pig oocytes after meiotic inhibition with a specific M-phase promoting factor kinase inhibitor, butyrolactone I. Biol Reprod 2002; 67:170–177.
34. Motlik J, Fulka J. Breakdown of the germinal vesicle in pig oocytes in vivo and in vitro. J Exp Zool 1976; 198:155–162.
35. Hyttel P, Madsen I. Rapid method to prepare mammalian oocytes and embryos for transmission electron microscopy. Acta Anat (Basel) 1987; 129:12–14.
36. Voit R, Schnapp A, Kuhn A, Rosenbauer H, Hirschmann P, Stunnenberg HG, Grummt I. The nucleolar transcription factor mUBF is phosphorylated by casein kinase II in the C-terminal hyperacidic tail which is essential for transactivation. EMBO J 1992; 11:2211–2218.
37. Hansen K, Farkas T, Lukas J, Holm K, Ronnstrand L, Bartek J. Phosphorylation-dependent and -independent functions of p130 cooperate to evoke a sustained G_1 block. EMBO J 2001; 20:422–432.
38. Wrenzycki C, Herrmann D, Carnwath JW, Niemann H. Alterations in the relative abundance of gene transcripts in preimplantation bovine embryos cultured in medium supplemented with either serum or PVA. Mol Reprod Dev 1999; 53:8–18.
39. Temeles GL, Ram PT, Rothstein JL, Schultz RM. Expression patterns of novel genes during mouse preimplantation embryogenesis. Mol Reprod Dev 1994; 37:121–129.
40. Shim C, Kwon HB, Kim K. Differential expression of laminin chain-specific mRNA transcripts during mouse preimplantation embryo development. Mol Reprod Dev 1996; 44:44–55.
41. Biggiogera M, Malatesta M, Abolhassani-Dadras S, Amalric F, Rothblum LI, Fakan S. Revealing the unseen: the organizer region of the nucleolus. J Cell Sci 2001; 114:3199–3205.
42. Hozak P, Cook PR, Schofer C, Mosgoller W, Wachtler F. Site of transcription of ribosomal RNA and intranucleolar structure in HeLa cells. J Cell Sci 1994; 107(pt 2):639–648.
43. Koberna K, Malinsky J, Pliss A, Masata M, Vecerova J, Fialova M, Bednar J, Raska I. Ribosomal genes in focus: new transcripts label the dense fibrillar components and form clusters indicative of ''Christmas trees'' in situ. J Cell Biol 2002; 157:743–748.
44. Cavanaugh AH, Hempel WM, Taylor LJ, Rogalsky V, Todorov G, Rothblum LI. Activity of RNA polymerase I transcription factor UBF blocked by Rb gene product. Nature 1995; 374:177–180.
45. Zatsepina OV, Bouniol-Baly C, Amirand C, Debey P. Functional and molecular reorganization of the nucleolar apparatus in maturing mouse oocytes. Dev Biol 2000; 223:354–370.
46. Ponderato N, Lagutina I, Crotti G, Turini P, Galli C, Lazzari G. Bovine oocytes treated prior to in vitro maturation with a combination of butyrolactone I and roscovitine at low doses maintain a normal developmental capacity. Mol Reprod Dev 2001; 60:579–585.
47. Ponderato N, Crotti G, Turini P, Duchi R, Galli C, Lazzari G. Embryonic and foetal development of bovine oocytes treated with a combination of butyrolactone I and roscovitine in an enriched medium prior to IVM and IVF. Mol Reprod Dev 2002; 62:513–518.
48. Marchal R, Tomanek M, Terqui M, Mermillod P. Effects of cell cycle dependent kinases inhibitor on nuclear and cytoplasmic maturation of porcine oocytes. Mol Reprod Dev 2001; 60:65–73.
49. Motlik J, Pavlok A, Kubelka M, Kalous J, Kalab P. Interplay between CDC2 kinase and MAP kinase pathway during maturation of mammalian oocytes. Theriogenology 1998; 49:461–469.
50. Lonergan P, Dinnyes A, Fair T, Yang X, Boland M. Bovine oocyte and embryo development following meiotic inhibition with butyrolactone I. Mol Reprod Dev 2000; 57:204–209.
51. Kubelka M, Anger M, Kalous J, Schultz RM, Motlik J. Chromosome condensation in pig oocytes: lack of a requirement for either cdc2 kinase or MAP kinase activity. Mol Reprod Dev 2002; 63:110–118.
52. Lohka MJ, Kyes JL, Maller JL. Metaphase protein phosphorylation in *Xenopus laevis* eggs. Mol Cell Biol 1987; 7:760–768.
53. Endo Y, Kopf GS, Schultz RM. Stage-specific changes in protein phosphorylation accompanying meiotic maturation of mouse oocytes and fertilization of mouse eggs. J Exp Zool 1986; 239:401–409.
54. Moor RM, Crosby IM. Protein requirements for germinal vesicle breakdown in ovine oocytes. J Embryol Exp Morphol 1986; 94:207–220.
55. Gall L, Le Gal F, De Smedt V. Protein phosphorylation patterns during in vitro maturation of the goat oocyte. Mol. Reprod. Dev. 1993; 36: 500–506.

56. Fulka J Jr, Leibfried-Rutledge ML, First NL. Effect of 6-dimethylaminopurine on germinal vesicle breakdown of bovine oocytes. Mol Reprod Dev 1991; 29:379–384.
57. Masui Y, Markert CL. Cytoplasmic control of nuclear behavior during meiotic maturation of frog oocytes. J Exp Zool 1971; 177:129–145.
58. Krischek C, Meinecke B. Roscovitine, a specific inhibitor of cyclin-dependent protein kinases, reversibly inhibits chromatin condensation during in vitro maturation of porcine oocytes. Zygote 2001; 9:309–316.
59. O'Mahony DJ, Xie WQ, Smith SD, Singer HA, Rothblum LI. Differential phosphorylation and localization of the transcription factor UBF in vivo in response to serum deprivation. In vitro dephosphorylation of UBF reduces its transactivation properties. J Biol Chem 1992; 267:35–38.
60. Voit R, Kuhn A, Sander EE, Grummt I. Activation of mammalian ribosomal gene transcription requires phosphorylation of the nucleolar transcription factor UBF. Nucleic Acids Res 1995; 23:2593–2599.
61. Klein J, Grummt I. Cell cycle-dependent regulation of RNA polymerase I transcription: the nucleolar transcription factor UBF is inactive in mitosis and early G_1. Proc Natl Acad Sci U S A 1999; 96: 6096–6101.
62. Voit R, Hoffmann M, Grummt I. Phosphorylation by G_1-specific cdk-cyclin complexes activates the nucleolar transcription factor UBF. EMBO J 1999; 18:1891–1899.